Parametric design of tri-axial nested Helmholtz coils

Jake J. Abbott[a)]
Department of Mechanical Engineering, University of Utah, Salt Lake City, Utah 84112, USA

(Received 5 March 2015; accepted 17 April 2015; published online 4 May 2015)

This paper provides an optimal parametric design for tri-axial nested Helmholtz coils, which are used to generate a uniform magnetic field with controllable magnitude and direction. Circular and square coils, both with square cross section, are considered. Practical considerations such as wire selection, wire-wrapping efficiency, wire bending radius, choice of power supply, and inductance and time response are included. Using the equations provided, a designer can quickly create an optimal set of custom coils to generate a specified field magnitude in the uniform-field region while maintaining specified accessibility to the central workspace. An example case study is included. © *2015 AIP Publishing LLC.* [http://dx.doi.org/10.1063/1.4919400]

I. INTRODUCTION

The term "Helmholtz coil" describes a pair of identical current-conducting coils arranged coaxially and with current flowing in the same direction (typically, the coils are connected in series to form a single circuit), which generates an optimally uniform magnetic field in the common central workspace of the coils.[1] Helmholtz coils are commonly used to generate fields to cancel the Earth's magnetic field, calibrate sensors, and perform a variety of other experiments in which a uniform magnetic field with controllable magnitude is desired. Due to symmetry, any pair of identical coaxial coils with the same current will have a field whose spatial derivative is zero in each direction at the center of the workspace. The field of a Helmholtz coil is optimally uniform in the sense that the spacing between the coils is chosen such that the second derivative in the axial direction is also zero. This definition results in a Helmholtz spacing between coils equal to 0.5 of the coil diameter (i.e., equal to the coil radius) in the case of circular coils[1] and 0.5445 of the coil width in the case of square coils.[2]

Many different aspects of the design and characterization of Helmholtz coils have been considered in prior work. Researchers have characterized the field generated by coils with non-zero cross section[1] and with coil asymmetry and non-ideal winding.[3] Others have analyzed the uniformity of the volume away from the central axis[4] and have considered changing the between-coil spacing from the Helmholtz spacing to expand the uniform-field region using a different definition of optimal uniformity.[5–7] Others have considered adding additional coils to improve the uniformity of the field.[8–10]

Tri-axial Helmholtz coils comprise three nested mutually orthogonal Helmholtz coils—inner, middle, and outer—each of which is designed as a traditional Helmholtz coil (potentially utilizing any of the modifications discussed above). The outer coils are larger than the middle, which in turn are larger than the inner, yet all three pairs are typically designed to generate the same magnitude of field in their common central uniform-field region. Each of the individual Helmholtz coils generates a uniform magnetic field parallel to its axis, and the three coils form a basis set such that a uniform field with controllable magnitude *and direction* can be established by controlling the three independent currents. Prior work has characterized how manufacturing and assembly errors affect the uniformity of the field in tri-axial coils.[13] There has been a significant recent interest in the use of tri-axial Helmholtz coils for the generation of magnetic fields for the control of "microrobots," both for applications under the guidance of an optical microscope,[11] as well as for applications in the human body.[12]

In each of the various projects that have used tri-axial Helmholtz coils, the respective research groups have redesigned the coils, starting from the basic spacing definition, such that their coils are customized to their specific needs in terms of magnitude of the field that can be generated, access to the central workspace (e.g., to place samples), access for imaging the central workspace (e.g., for a microscope lens), the current amplifiers required, and the size and cost of the final system. This perpetual redesign harms productivity, particularly considering that the design of tri-axial Helmholtz coils is a well-constrained problem that has simply never been elucidated.

The intent of this paper is to eliminate the aforementioned inefficiency and provide a simple set of design equations and guidelines that will enable researchers to quickly design a set of custom tri-axial Helmholtz coils for their specific needs, specified in terms of field strength and workspace-access dimensions. Both circular-coil and square-coil systems are described. This paper focuses only on the design of the coils themselves and does not describe the supporting structure that will be needed to maintain the coils in their intended positions, which can take many forms. This paper is structured as follows. Section II begins with the design assumptions used to limit the optimization problem to a tractable one. Section III describes some practical considerations when fabricating coils from insulated magnet wire. Sections IV and V then present the geometric design of circular-coil and square-coil systems, respectively. Section VI characterizes the power requirements, the choice of current density, and the inductance (and the resulting time response) for a given design. A succinct model

a)Electronic mail: jake.abbott@utah.edu

for the inductance of a Helmholtz coil, which is not currently available in the literature, is another contribution of this paper. Finally, Sec. VII presents a case study illustrating the complete design process of a set of tri-axial Helmholtz coils, starting with a typical set of design specifications.

II. ASSUMPTIONS

Let us begin with a set of reasonable simplifying assumptions to guide our parametric design.

(1) Although we consider both circular and square coils, we only consider coils with square cross section.
(2) When calculating the field generated in the center of the uniform-field region, we assume that the entire current flowing through the coil's square cross section can be modeled as flowing through the center of the coil's square cross section.
(3) We only consider the spacing of true Helmholtz coils, measured from the centers of the coil cross sections.
(4) We assume that each of the three coil pairs has the same limit on maximum current density, which is typically governed by Joule heating concerns.
(5) We assume that each of the three coil pairs should generate the same magnitude of magnetic field in the center of the workspace, given the same current density (i.e., our tri-axial coils should have no special directions).
(6) We assume that it is desirable that the coils be as compact as possible. That is, once an inner coil pair is designed, the middle coil pair is designed to be as small as possible while meeting all other design constraints, which will result in direct contact of the middle coil with the inner coil and similarly from the middle coil pair to the outer coil pair.
(7) We assume that the coils are to be used in quasistatic (low-frequency) modes, such that high-frequency effects, such as skin effect, can be neglected.
(8) A spool is often used to wind and constrain the coils. The spool wall thicknesses will typically be governed by considerations related to strength, manufacturability, and material availability and are largely outside of the electromagnet design process. We assume the spool wall thicknesses are given.

III. WIRE PACKING EFFICIENCY

Before designing the geometry of our coils, we must first understand the nature of the insulated magnet wire that is used in coil fabrication and the packing efficiency that we can reasonably expect to obtain. That is, for a coil cross section of dimensions $X_c \times X_c$, we would like to determine what fraction of cross section will actually be conductor (e.g., copper) by accounting for insulation and voids inherent to the wire and the wrapping.

Common choices of insulated magnet wire include circular, square, and flat/ribbon wire. We will only consider circular and square wire here, since it is difficult with flat/ribbon wire to design the type of optimized coils that are the subject of this paper. Figure 1 shows the parameters that are used to define the geometry of the wire's cross section, including the bounding box of coil's cross-sectional area taken up by a single wire. Note that because of the alternating handedness of the helical pitch of the wire from one layer to the next when winding a coil, denser packing is not typically achieved even with the circular wire.

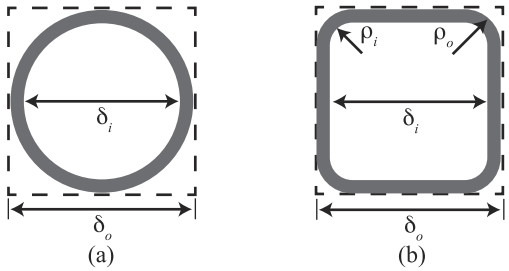

FIG. 1. Geometric parameters describing insulated wire cross sections, with wires shown inside their bounding areas (as dashed lines). (a) Parameters for circular wire, with outer diameter δ_o and inner (conductor) diameter δ_i. (b) Parameters for square wire, with outer dimensions $\delta_o \times \delta_o$ with corner radius-of-curvature ρ_o, and inner (conductor) dimensions $\delta_i \times \delta_i$ with corner radius-of-curvature ρ_i.

For circular wire, the packing efficiency is calculated using Fig. 1(a) as the ratio of the conducting area of the wire relative to its bounding box,

$$\epsilon = \frac{\pi \delta_i^2}{4\delta_o^2}. \tag{1}$$

Similarly for square wire, the packing efficiency is calculated using Fig. 1(b) and Appendix A as the ratio of the conducting area of the wire relative to its bounding box,

$$\epsilon = \frac{\delta_i^2 - 0.8584\rho_i^2}{\delta_o^2}. \tag{2}$$

For both wire types, the insulation's thickness is simply

$$t = \frac{\delta_o - \delta_i}{2}. \tag{3}$$

The geometry-based values in (1) and (2) overestimate the true packing efficiency. We must also acknowledge that the helical pitch of wire as it is wrapped in a given layer of the coil results in further reduction in packing efficiency. For a given layer of wire in a coil, we lose a full wire dimension δ_o, that is, n full turns of tightly packed wire result in a coil width of approximately $(n+1)\delta_o$, rather than $n\delta_o$, due to the helical pitch of the wrap.

A simple way to account for the reduction in packing efficiency when calculating the generated magnetic field is to consider an effective coil cross section dimension $(X_c - \delta_o) \times (X_c - \delta_o)$, which requires no modification to the value for ϵ calculated above. This effective coil cross section dimension is accurate in the axial direction of the coil and is conservative in the radial direction of the coil since the integer number of wire layers can result in a discrepancy of up to δ_o from any arbitrary intended X_c (assuming we will never add an additional layer of wire that would cause the coil to exceed its intended size).

When calculating the total length of wire required and the resulting wire resistance, the above simplification would not be conservative. When calculating electrical parameters, we will

use the above simplification only in the axial direction of the coil and will explicitly calculate the integer number of wraps in the radial direction.

IV. DESIGN OF CIRCULAR COILS

We will begin with the design of circular coils. The geometry and parameters of the Helmholtz coil being considered are shown in Fig. 2. The nominal diameter of the coils is D_c (all lengths in units m), measured from the center of the square cross section, where we will use the subscript $c \in \{1,2,3\}$ to designate the first (inner), second (middle), and third (outer) Helmholtz coils. The square cross sections of the respective coils are described by the length X_c. The coils are assumed to be wrapped on a spool with an inner-wall thickness of S_c and a side-wall thickness of T_c; our development generalizes to the case when there is no spool (i.e., $S_c = T_c = 0$). For circular Helmholtz coils, the two coils within a pair have a nominal separation distance equal to 0.5 of the nominal diameter. These variable definitions lead directly to definitions for the inner diameter

$$D_{ic} = D_c - X_c - 2S_c, \tag{4}$$

the outer diameter

$$D_{oc} = D_c + X_c, \tag{5}$$

and the gap between individual coils within a given Helmholtz coil pair

$$G_c = 0.5D_c - X_c - 2T_c. \tag{6}$$

We can conduct the rest of the design as a function of a single variable: X_1. Once this cross section dimension of the inner coil is established, the resulting geometry of the remainder of the tri-axial Helmholtz coils follows directly. We can then optimize our design over X_1 in order to achieve our given design specifications while minimizing some metric such as size or cost.

The magnitude of the uniform magnetic field (in units A m^{-1}), or more specifically in the center of the uniform-field region, generated by a given Helmholtz coil with a current density J (in units A m^{-2}) in the conducting portion of the wire and a wire-packing efficiency ϵ can be found by utilizing the Biot-Savart law integrated over the two individual coils,[1] utilizing assumption (2) from Sec. II. The field magnitude is given by

$$H = \frac{1.43J\epsilon(X_c - \delta_o)^2}{D_c}, \tag{7}$$

where $\epsilon(X_c - \delta_o)^2$ is the effective conducting coil cross section of a given coil discussed in Sec. III and $J\epsilon(X_c - \delta_o)^2$ is the total circulating current in a given coil. We must maintain this value of H for all three coils sets. Note that we could also express equations for the magnetic field in terms of the flux density $B = \mu_0 H$ in units T, where $\mu_0 = 4\pi \times 10^{-7}$ T m A^{-1} is the permeability of free space.

Given a desired value of H, we can rearrange (7) to express D_c as a function of known parameters,

$$D_c = \left(\frac{1.43J\epsilon}{H}\right)(X_c - \delta_o)^2 = \xi(X_c - \delta_o)^2, \tag{8}$$

where ξ is constant across all three coil sets. Thus, for a given value of X_1, the nominal diameter D_1 is computed above, and the resulting inner coil diameter D_{i1}, outer coil diameter D_{o1}, and gap size G_1 can be calculated by (4), (5), and (6), respectively.

With the complete geometry of the first coil set established, we can solve for the geometry of the second coil set based on the first and then the third based on the second. The equation for D_c as a function of X_c provided in (8) applies to all three coil sets, but in the case of the second and third set, X_c is not known *a priori*. When circular Helmholtz coils with square cross section are tightly nested, the innermost edge of the second coil comes into contact with the outermost edge of the first coil, with an analogous relationship between the second and third coils (this can be visualized in Fig. 3). This

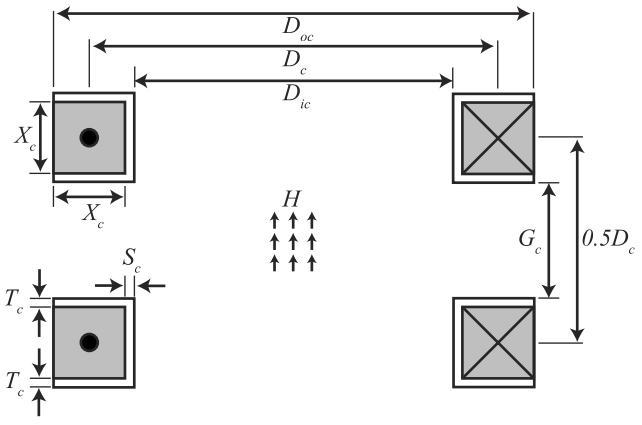

FIG. 2. Geometric parameters defining circular Helmholtz coils with square coil cross section. For current flowing through the cross section in the direction indicated, a uniform field H is generated in the common center of the coils in the direction indicated.

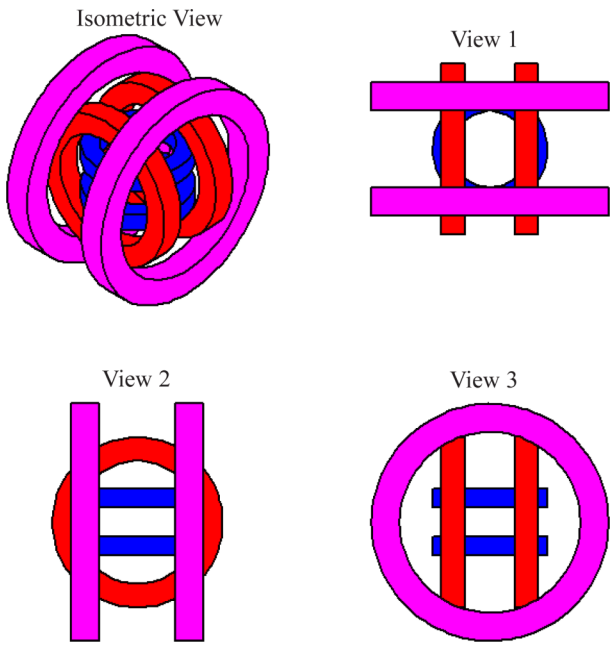

FIG. 3. Example tri-axial Helmholtz coil design with circular coils ($S = T = \delta_o = 0$, $\xi = 500\,\mathrm{m}^{-1}$, and $X_1 = 0.01$ m).

provides the constraint equation

$$D_{oc-1}^2 - G_c^2 = D_{ic}^2 - (G_{c-1} + 2X_{c-1} + 4T_{c-1})^2 \qquad (9)$$

for $c \in \{2,3\}$. With the geometry of the first coil already established, combining the constraints in (4), (6), and (9) results in a quartic equation of X_c, for which we must solve for its single positive real root (more detail is provided in Appendix B). With the solution for X_c found, we can solve for the accompanying nominal coil diameter D_c using (8). The resulting inner coil diameter D_{ic}, outer coil diameter D_{oc}, and gap size G_c can then be calculated by (4), (5), and (6), respectively. This process is used to solve for all of the parameters for the middle Helmholtz coil ($c = 2$) and then repeated for the outer Helmholtz coil ($c = 3$).

The central workspace can be accessed from three different views as shown in Fig. 3, where view c is coaxial with Helmholtz coil c. The view-1 access window is the intersection of a rectangle of dimension $G_2 \times G_3$ with a circle of diameter D_{i1}. The view-2 access window is a rectangle with dimensions $G_1 \times G_3$ and the view-3 access window is a rectangle with dimensions $G_1 \times G_2$.

A final design consideration is the minimum radius-of-curvature in the coils. For a given wire, the manufacturer will provide a minimum radius-of-curvature that is allowable in the wire without risk of damage to the wire or its insulation. We must ensure that the minimum radius-of-curvature in our coils is greater than that value. The minimum radius-of-curvature is in the first wrap of any given coil, with a value of

$$r_{\min,c} = \frac{D_{ic}}{2} + S_c. \qquad (10)$$

The inner coil ($c = 1$) will have the smallest minimum radius-of-curvature.

In summary, given a choice of H, ϵ, J, S, and T, the complete design of the geometry of the electromagnets themselves can be expressed as a function of a single variable: X_1. The choice for this parameter should be made as small as possible (which will result in all X_c and D_c values being as small as possible) while still providing some desired level of access to the central workspace. It should be noted that the wrapping-efficiency equations of Sec. III fundamentally assume that the coil comprises at least one complete turn of wire, so only values of $X_1 \geq 2\delta_o$ should be considered. In addition, any value of X_1 that results in a calculated $D_{i1} < 0$ is an invalid choice of X_1 and will lead to nonsensical results. Figure 3 depicts an example tri-axial Helmholtz coil designed with equations above. A case study illustrating the complete design process is provided in Sec. VII.

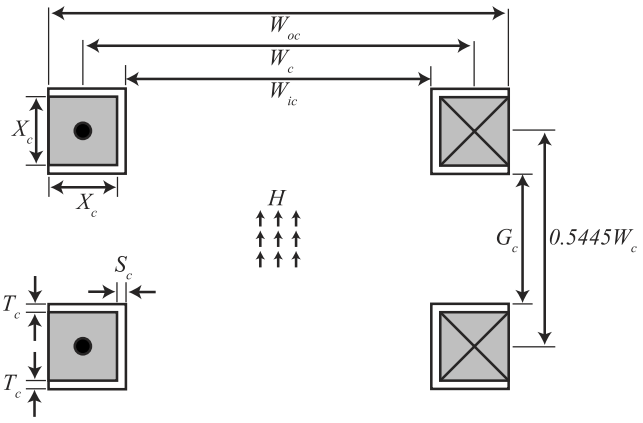

FIG. 4. Geometric parameters defining square Helmholtz coils with square coil cross section. For current flowing through the cross section in the direction indicated, a uniform field H is generated in the common center of the coils in the direction indicated.

V. DESIGN OF SQUARE COILS

Let us now repeat the design process for square coils, with a small amount of repetition from Sec. IV for clarity. The geometry and parameters of the Helmholtz coil being considered are shown in Fig. 4. The nominal width of the coils is W_c, measured from the center of the square cross section. The square cross sections of the respective coils are described by the length X_c. The coils are assumed to be wrapped on a spool with an inner-wall thickness of S_c and a side-wall thickness of T_c. For square Helmholtz coils, the two coils within a pair have a nominal separation distance equal to 0.5445 of the nominal width. These variable definitions lead directly to definitions for the inner width

$$W_{ic} = W_c - X_c - 2S_c, \qquad (11)$$

the outer width

$$W_{oc} = W_c + X_c, \qquad (12)$$

and the gap between individual coils within a given Helmholtz coil pair

$$G_c = 0.5445W_c - X_c - 2T_c. \qquad (13)$$

We can conduct the rest of the design as a function of a single variable: X_1. Once this cross section dimension of the inner coil is established, the resulting geometry of the remainder of the tri-axial Helmholtz coils follows directly. We can then optimize our design over X_1.

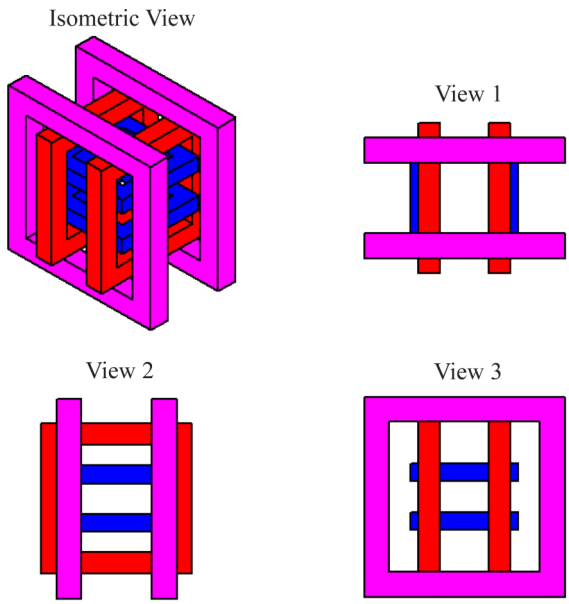

FIG. 5. Example tri-axial Helmholtz coil design with square coils ($S = T = \delta_o = 0$, $\xi = 500\,\mathrm{m}^{-1}$, and $X_1 = 0.01$ m).

The magnitude of the uniform magnetic field generated by a given Helmholtz coil with a current density J in the conductor and a wire-packing efficiency ϵ is given by

$$H = \frac{1.30J\epsilon(X_c - \delta_o)^2}{W_c}, \tag{14}$$

where $\epsilon(X_c - \delta_o)^2$ is the effective conducting coil cross section discussed in Sec. III and $J\epsilon(X_c - \delta_o)^2$ is the total circulating current.[2] We must maintain this value of H for all three coil sets.

Given a desired value of H, we can rearrange (14) to express W_c as a function of known parameters,

$$W_c = \left(\frac{1.30J\epsilon}{H}\right)(X_c - \delta_o)^2 = \xi(X_c - \delta_o)^2, \tag{15}$$

where ξ is constant across all three coil sets. Thus, for a given value of X_1, the nominal width W_1 is computed above, and the resulting inner coil width W_{i1}, outer coil width W_{o1}, and gap size G_1 can be calculated by (11), (12), and (13), respectively.

With the complete geometry of the first coil set established, we can solve for the geometry of the second coil based on the first and then the third based on the second. The equation for W_c as a function of X_c provided in (15) applies to all three coil sets, but in the case of the second and third set, X_c is not known *a priori*. The geometry of nested square Helmholtz coils is simple relative to that of nested circular Helmholtz coils: the inner width of the second coil should be equal to the outer width of the first coil, with an analogous relationship between the second and third coils (this can be visualized in Fig. 5). This provides the constraint equation

$$W_{ic} = W_{oc-1} \tag{16}$$

for $c \in \{2,3\}$. Combining (11), (15), and (16), we arrive at an equation for X_c based on known quantities,

$$X_c = \delta_o + \frac{1}{2\xi}\Big(1 + \big((1 + 2\xi\delta_o)^2 - 4\xi(\xi\delta_o^2 - W_{ic} - 2S_c)\big)^{1/2}\Big) \tag{17}$$

for $c \in \{2,3\}$. The nominal coil width W_c can then be computed using (15) and the resulting outer coil width W_{oc} and gap size G_c can be calculated with (12) and (13), respectively. This process is used to solve for all of the parameters for the middle Helmholtz coil ($c = 2$) and then repeated for the outer coil ($c = 3$).

The central workspace can be accessed from three different views as shown in Fig. 5, where view c is coaxial with Helmholtz coil c. The view-1 access window is the intersection of a rectangle of dimension $G_2 \times G_3$ with a square of side-length W_{i1}. The view-2 access window is a rectangle with dimensions $G_1 \times G_3$ and the view-3 access window is a rectangle with dimensions $G_1 \times G_2$.

A final design consideration is the minimum radius-of-curvature in the coils. This is a more critical consideration in the case of square coils than it is in the case of circular coils. In practice, we will never construct a true square coil because the wire cannot follow the perfect 90° bend at the corner. Rather, we will need to round the corners. For a given wire, the manufacturer will provide a minimum radius-of-curvature that is allowable in the wire without risk of damage to the wire or its insulation; we must ensure that the minimum radius-of-curvature in our coils is greater than that value. The simplest method for rounding the corners is a circular profile with radius-of-curvature Δ_c. The circular corner profile results in a minimum radius-of-curvature in the wire of

$$r_{\min,c} = \Delta_c + S_c \tag{18}$$

for $c \in \{1,2,3\}$. The values of Δ_c should be chosen to round the corners of the coils gently enough to ensure that no damage is done to the wire during wrapping, yet not so large that the access to the central workspace is significantly hindered. Some mechanical constraint must also be put in place to avoid bowing in the coils. In the case of the inner coil, the radius-of-curvature is restricted to be, at most, half of the inner width,

$$\Delta_1 = 0.5W_{i1}. \tag{19}$$

However, choosing Δ_1 this large would effectively turn the inner Helmholtz coil into a circular Helmholtz coil. In the case of the middle and outer coils, the maximum allowable radius-of-curvature is more restricted so as to not conflict with the next-smaller coil; this is described in detail in Appendix C.

Rounding the corners of a nominally square Helmholtz coil will have a small effect on the uniform-field region. For a given Helmholtz coil, if we were to continuously increase the radius-of-curvature at the corners from zero up to the maximum allowable value described in (19), we would observe a continuous evolution of the uniform-field region from that of a square Helmholtz coil to that of a circular Helmholtz coil, both of which have been characterized in prior work (see Sec. I).

VI. ELECTRICAL DESIGN CONSIDERATIONS

A. Power

To calculate the power requirements for circular and square coils, we begin by finding the effective volume of wire in a single coil, accounting for the wire-wrapping modification in the axial direction discussed in Sec. III and accounting for the integer number of wire layers in the radial direction. For a circular coil, the effective volume can be calculated as the volume of a large disk minus the volume of a small disk, each with a width in the axial direction of $(X_c - \delta_o)$,

$$\Psi_c = \frac{\pi}{4}(X_c - \delta_o)\left(D_{ic} + 2S_c + 2\delta_o\left\lfloor\frac{X_c}{\delta_o}\right\rfloor\right)^2 - \frac{\pi}{4}(X_c - \delta_o)(D_{ic} + 2S_c)^2, \tag{20}$$

where $\lfloor x \rfloor$ is the floor function that returns the largest integer that is less than or equal to x, which is used to calculate the maximum integer number of wire wraps that can fit within a given X_c in the radial direction of the coil. For a square coil, the effective volume is

$$\Psi_c = (X_c - \delta_o)\left(W_{ic} + 2S_c + 2\delta_o\left\lfloor\frac{X_c}{\delta_o}\right\rfloor\right)^2 - (X_c - \delta_o)(W_{ic} + 2S_c)^2. \tag{21}$$

Note that these volumes are each for a single coil within a Helmholtz coil pair. Also note that (21) does not account for any rounding of the coil's square corners, making it a conservative overestimate of the effective volume.

The remaining equations assume that the two coils within a Helmholtz pair are connected in series and powered using a single amplifier, as is typical. Using the cross section of the bounding box of a single wire (see Fig. 1), we can estimate the total length of wire, λ_c, in a Helmholtz coil as

$$\lambda_c = \frac{2\Psi_c}{\delta_o^2}. \tag{22}$$

A resistance per unit length η (in units $\Omega\ \mathrm{m}^{-1}$) is used to estimate the resistance (in units Ω) of the Helmholtz coil,

$$R_c = \eta \lambda_c. \tag{23}$$

For a given desired current density J, we can calculate the current required for a given wire choice (see Fig. 1 for conductor cross-sectional area). For circular wire,

$$I = \frac{\pi \delta_i^2}{4} J \tag{24}$$

and for square wire, utilizing Appendix A,

$$I = \left(\delta_i^2 - 0.8584\rho_i^2\right) J. \tag{25}$$

The voltage (in units V) required to generate the desired current is then calculated as

$$V_c = I R_c \tag{26}$$

and the power (in units W) delivered is calculated as

$$P_c = I^2 R_c = I V_c. \tag{27}$$

B. Current density *J*

The field magnitude is linearly proportional to the current density J, so it is clear that we should choose a current density as large as possible without causing any problems related to heat generation, in order to keep the size of the coils to a minimum. Mitigating problems related to heat generation typically means ensuring that the wire's insulation is not at risk of breaking down, using limits provided by the wire manufacturer. However, it can also be further limited by the specific application of the coils (e.g., in microbiology).

Heat generation/dissipation is a complex function of coil geometry and coil cooling and cannot be summarized in a simple way. There are a number of rules-of-thumb values used for electrical wiring and the design of electrical machines that can be found in a variety of sources. Conservative rules-of-thumb for current density that assume the wire is fully embedded typically use values of 2 $\mathrm{A/mm^2}$ or 2.5 $\mathrm{A/mm^2}$. Rules-of-thumb for exposed wire with free-convection cooling typically use values of 6 $\mathrm{A/mm^2}$, but the size of the wire (i.e., the ratio of surface area to volume) will affect the heat dissipation. Even a small amount of forced cooling can enable substantial increases in allowable current density. The author's lab has successfully used 6 $\mathrm{A/mm^2}$ in tri-axial Helmholtz coils with a small desk fan for cooling.[14] Knowledge of the duty cycles of the coils can also be used to increase the allowable *instantaneous* current density.

C. Inductance and time response

The inductance L_c of a Helmholtz coil combined with the resistance of the Helmholtz coil determines the coil's time response. We can compute a time constant as

$$\tau_c = \frac{L_c}{R_c}, \tag{28}$$

where R_c is the resistance of the pair connected in series. For a sinusoidal input of frequency ω rad s^{-1}, we can compute the attenuation gain $M_c(\omega)$ and phase lag $\phi_c(\omega)$ of the output signal from that desired as

$$M_c(\omega)\angle\phi_c(\omega) = \frac{1}{1 + \tau_c \omega \sqrt{-1}}. \tag{29}$$

Note that when coils are driven using current-control amplifiers, rather than voltage-control, the values in (28) and (29) describe a conservative (i.e., worst-case) time response that applies only to the largest current commands.

The inductance of the Helmholtz coil is calculated as a function of the self-inductance and the mutual inductance of the individual coils,

$$L_c = 2L_{\mathrm{self},c} + 2L_{\mathrm{mut},c}. \tag{30}$$

Note that the inductance L_c of a given Helmholtz coil has no mutual inductance with either of the other two Helmholtz coils in the tri-axial nested system, due to the Helmholtz coils being arranged orthogonally and symmetrically. Any flux passing through one of the individual coils in a given Helmholtz pair generated by any of the orthogonal coils will be accompanied by an equal-but-opposite flux in the other individual coil in the given Helmholtz pair (recall that the two individual coils are connected in series).

1. Inductance of circular coils

To calculate the self-inductance of a circular coil (in units H), we will make use of a simple empirical approximation given by Wheeler,[15]

$$L_{\mathrm{circ}}(\alpha, \beta, \gamma) = \frac{(7.9 \times 10^{-6})\alpha^2 n^2}{3\alpha + 9\beta + 10\gamma}, \tag{31}$$

where α is the nominal diameter of the coil, β is the length of the coil cross section in the axial direction, γ is the length of the coil cross section in the radial direction, and n is the number of turns in the coil cross section, which we will calculate for a given wire choice with outer dimension δ_o as

$$n(\beta, \gamma) = \left(\frac{\beta - \delta_o}{\delta_o}\right)\left\lfloor \frac{\gamma}{\delta_o} \right\rfloor, \tag{32}$$

where the leftmost quantity represents the real number of turns in the axial direction and the rightmost quantity represents the integer number of turns in the radial direction. We can then calculate the self-inductance of one coil in our Helmholtz pair as

$$L_{\mathrm{self},c} = L_{\mathrm{circ}}(D_c, X_c, X_c) \tag{33}$$

which can then be applied to (30). To calculate the $2L_{\mathrm{mut},c}$ term in (30), we will make use of an exact equivalence for two identical coaxial coils provided by Grover,[16] which utilizes

self-inductance and superposition, and we will incorporate knowledge of the Helmholtz separation distance,

$$\begin{aligned} 2L_{\text{mut},c} = {} & L_{\text{circ}}(D_c, 0.5D_c + X_c, X_c) \\ & + L_{\text{circ}}(D_c, 0.5D_c - X_c, X_c) \\ & - 2L_{\text{circ}}(D_c, 0.5D_c, X_c). \end{aligned} \tag{34}$$

We can now calculate the inductance of a Helmholtz pair, connected in series, using (30).

In Appendix D, we compare the estimation method above to experimentally determined values from prior work. We conclude that this estimate of inductance will suffice for the purpose of our design process, with the understanding that a factor of safety should be included if coil time response is critical.

2. Inductance of square coils

To approximate the self-inductance of a square coil (in units H), we will simply modify the empirical approximation in (31) by $4/\pi$ to account for the difference in flux area between a square coil and a circular coil,

$$L_{\text{square}}(\alpha, \beta, \gamma) = \frac{(1.0 \times 10^{-5})\alpha^2 n^2}{3\alpha + 9\beta + 10\gamma}, \tag{35}$$

where α is now the nominal width of the coil, β is the length of the coil cross section in the axial direction, γ is the length of the coil cross section in the width direction, and n is the number of turns in the coil cross section, which we can calculate using (32). We can then calculate the self-inductance of one coil in our Helmholtz pair as

$$L_{\text{self},c} = L_{\text{square}}(W_c, X_c, X_c) \tag{36}$$

which can then be applied to (30). To calculate the $2L_{\text{mut},c}$ term in (30), we will again make use of the exact equivalence provided by Grover,[16] combined with knowledge of the Helmholtz separation distance,

$$\begin{aligned} 2L_{\text{mut},c} = {} & L_{\text{square}}(W_c, 0.5445W_c + X_c, X_c) \\ & + L_{\text{square}}(W_c, 0.5445W_c - X_c, X_c) \\ & - 2L_{\text{square}}(W_c, 0.5445W_c, X_c). \end{aligned} \tag{37}$$

We can now calculate the inductance of a Helmholtz pair, connected in series, using (30). Again, this inductance calculation should be viewed as an approximation that is suitable for coil design but that should include a small factor of safety if time response is critical. The inductance calculation above does not account for any rounding of the corners and can thus be considered a conservative estimate, since rounding the corners will tend to reduce the inductance.

VII. THE DESIGN PROCESS: A CASE STUDY

Let us carry out a case study demonstrating how the methods and equations presented in this paper can be used to design a set of tri-axial Helmholtz coils. A given design is highly dependent on the choice of wire. However, once a wire is chosen, the equations in this paper, incorporated into a numerical package such as MATLAB, can be used to quickly generate the optimal design for that specific wire choice. This process can be repeated for a small set of possible wire choices (e.g., from a list of available wire from a given manufacturer), and then, the best wire choice can be made given some other design specification (e.g., cost, size, and power-amplification requirements).

In this case study, which is intended for tutorial purposes, all design specification used are arbitrary and only chosen to illustrate the design process. We would like to create a set of coils for an application under the guidance of an optical microscope. We have a number of design specifications.

(1) We would like to generate a maximum field strength of $B = 10\,\text{mT}$, which we convert to H by dividing by the permeability of free space μ_0, giving $H = 7958\,\text{A m}^{-1}$.
(2) We are willing to pay a premium cost for square wire, which will give us a packing efficiency that is better than with circular wire. To constrain our design space, we will choose our wire exclusively from the catalogue of MWS Wire Industries.
(3) We will construct circular coils, due to their relative simplicity in fabrication. We could also repeat the process for square coils and compare the optimal square-coil system to the optimal circular-coil system but that will be omitted here for brevity.
(4) We will fabricate our own spools on which to wind the coils, with $S_c = 0.004\,\text{m}$ and $T_c = 0.003\,\text{m}$.
(5) We would not like the coils to be in any danger of overheating, so we will use a conservative current density of $J = 2.5 \times 10^6\,\text{A m}^{-2}$.
(6) We will connect our respective Helmholtz-coil pairs in series as is typical, so that we only need three current-controlled amplifiers (rather than six for independent coil control).
(7) To constrain our design, we will choose our power supply and current amplifiers exclusively from those available from Advanced Motion Controls.
(8) The microscope lens, which views the workspace from the top down, has a lens with a diameter of 3 cm. We will arrange the tri-axial coils so that the top-down view is view 1. This provides constraints for $G_2 \geq 0.03\,\text{m}$, $G_3 \geq 0.03\,\text{m}$, and $D_{i1} \geq 0.03\,\text{m}$.
(9) We would like a workspace access window from the side that is at least 2 cm tall and 4 cm wide, but we do not care if the access is from view 2 or view 3. The 2-cm specification provides the constraint $G_1 \geq 0.02\,\text{m}$. The 4-cm specification requires that either $G_2 \geq 0.04\,\text{m}$ or $G_3 \geq 0.04\,\text{m}$.
(10) For good practice, all of the above access specifications already include a small factor of safety, as does the desired magnetic field strength.

For brevity, we will conduct a design and report values for only a few wire gauges: 12 AWG, 14 AWG, and 16 AWG. We will first go through the complete design process to find the optimal coil geometry for the 12 AWG wire. Figure 6 shows the set of possible geometries, as a factor of the free parameter X_1, that will result in the desired field strength in each direction, for 12 AWG wire. Our goal is to choose X_1 as small as possible while meeting all of our workspace-access

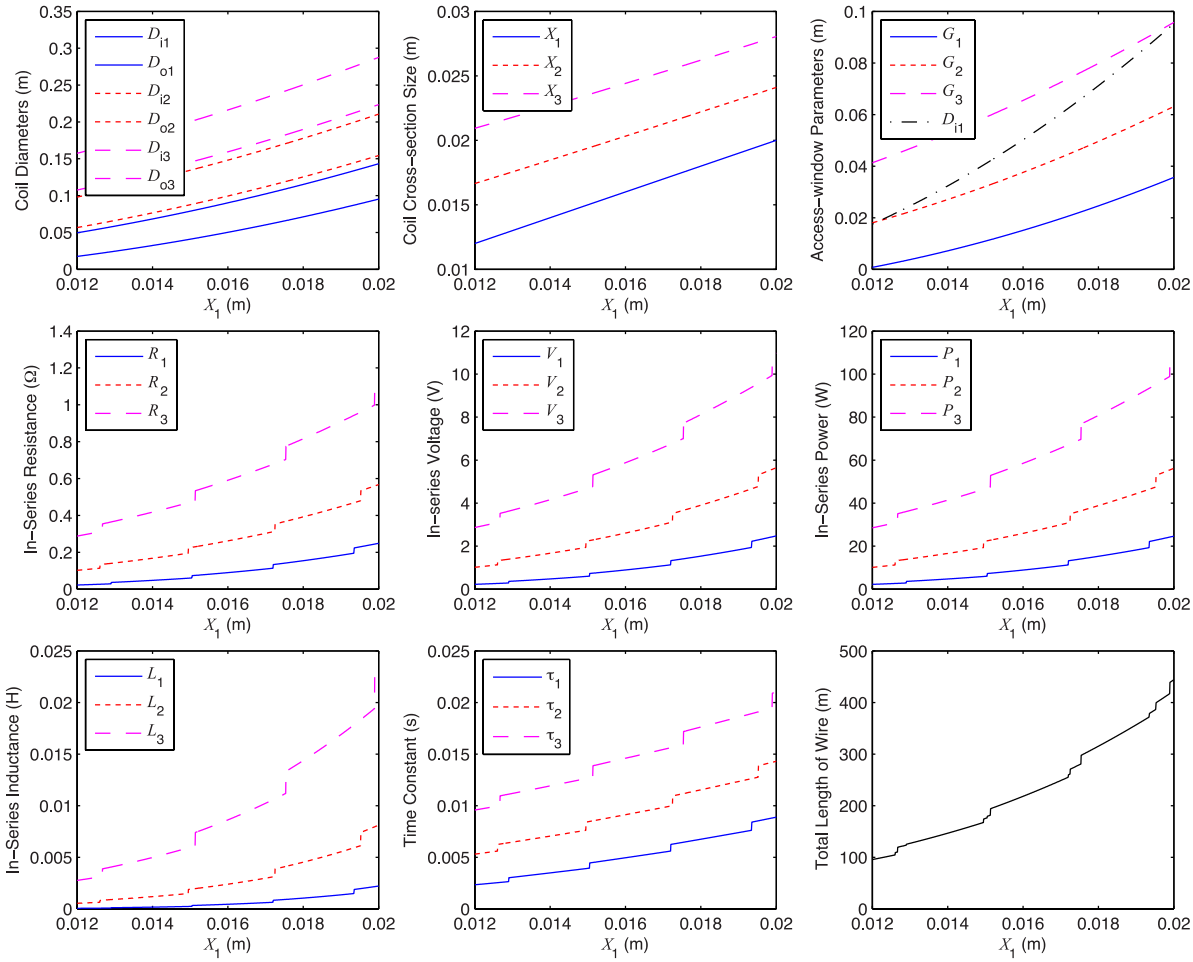

FIG. 6. Tri-axial nested coil designs for a range of X_1 that achieve the desired field strength with the desired current density in the case study, using 12 AWG square wire. $X_1 = 0.0171$ m is the smallest value of X_1 that achieves the design specifications of the case study.

specifications. We see that choosing X_1 as small as possible will ultimately result in the smallest coils that will satisfy our needs and will result in a minimal material cost, as observed in the total length of wire that will be required. We find that the smallest possible X_1 that will satisfy all of our geometric specifications is $X_1 = 17.1$ mm for 12 AWG wire.

The complete results of this *optimal* 12 AWG design are shown in Table I, along with the results for the two other wire gauges under consideration, obtained using the same process just described. As we look at the results, a few rules-of-thumb for coil design become clear. First, of the three Helmholtz coils, the third (outer) Helmholtz coil dominates the design, demanding the most voltage and power to generate a field in its axial direction and resulting in the slowest time response. Thus, we can use the values from the third coil exclusively in our selection process. Second, the coil geometries,

TABLE I. Optimal design parameters for circular tri-axial Helmholtz coils, for three square wire gauges, for the design specifications in the case study. The parameters δ_i, δ_o, ρ_i, and η are average values from the manufacturer's data sheets (MWS Wire Industries). The parameters I, λ_c, R_c, V_c, P_c, L_c, and τ_c are calculated for the given coil pair connected in series.

Gauge (AWG)	δ_i (mm)	δ_o (mm)	ρ_i (μm)	η (mΩ/m)	I (A)	Coil pair	X_c (mm)	D_{ic} (mm)	D_c (mm)	D_{oc} (mm)	G_c (mm)	λ_c (m)	R_c (Ω)	V_c (V)	P_c (W)	L_c (mH)	τ_c (ms)
						1	17.1	61.1	86.2	103	20.0	25.7	0.111	1.11	11.0	0.614	5.53
12	2.05	2.15	508	4.32	9.95	2	21.3	113	142	164	43.8	70.8	0.306	3.04	30.3	3.02	9.88
						3	25.4	175	209	234	73.0	155	0.668	6.65	66.2	10.4	15.5
						1	16.8	60.8	85.6	102	20.0	41.5	0.285	1.79	11.3	1.57	5.50
14	1.63	1.73	406	6.87	6.29	2	21.1	112	141	162	43.5	119	0.815	5.13	32.2	8.29	10.2
						3	25.1	174	207	232	72.3	245	1.68	10.6	66.6	25.9	15.4
						1	16.5	60.5	85.0	101	20.0	62.8	0.716	2.88	11.6	3.58	5.01
16	1.29	1.39	254	11.4	4.02	2	20.7	111	140	160	43.1	169	1.93	7.76	31.2	17.2	8.91
						3	24.8	172	205	229	71.5	366	4.17	16.8	67.4	58.2	14.0

TABLE II. Options for "300 W" power supplies with 120 VAC input voltage from Advanced Motion Controls.

Model	DC output voltage (VDC)	Output current (A)
PS4X3W24	24	12
PS4X3W48	48	6

power required, and time response are primarily dictated by the desired field strength and the workspace-access specifications and are largely independent of the wire gauge, with only small differences that will not significantly affect our wire selection. Third, the choice of wire gauge will largely come down to a trade-off between voltage and current used to power the coils.

We choose a wire gauge based on available power supplies. We will choose from the PS4X series of power supplies from Advanced Motion Controls (Table II). These power supplies can be used to power all three of our required current drives from a single supply. We will only consider those drives that use 120 VAC input, but higher-voltage/lower-current options are available if we are able to use 240 VAC input. The 288 W available from the power supply is much larger than the 66.2 W required. Assuming that we do not decide to search for a smaller and potentially less expensive power supply, this would be a good opportunity to reconsider the original design specifications, in order to arrive at a better set of tri-axial Helmholtz coils than what was originally specified. What should we improve? Would we like to generate a stronger field? Would we like easier access to the central workspace? Or, are our original specifications good enough, and would we really just like as fast a time response as possible? The answers to these questions will enable us to iterate our design if desired.

Based on our design specifications, it appears that the best choice is the PS4X3W24 power supply with the 12 AWG wire. The 12 A of current is sufficient to generate the required 9.95 A with a small factor of safety. The 24 V is nearly four times larger than the required 6.65 V, which will positively affect the time response of the coils (note that 6.65 V is the voltage required to command a *steady-state* current of 9.95 A, but the coil's inductance will demand the maximum voltage during the entire transient response when the amplifiers are driven in a current-control mode). For brevity, we will stop with this choice, but based on the values for current, voltage, and time constant calculated for 14 AWG and 16 AWG wires, it would be advisable to calculate the values for 15 AWG to be used in conjunction with the PS4X3W48 supply. Since the total length of wire is also calculated for each of the designs, a final decision could be influenced by the cost of specific wire. When hand-wrapping coils, choosing a larger wire gauge can make the task easier.

VIII. CONCLUSIONS

This paper provided an optimal parametric design for tri-axial nested Helmholtz coils. Circular and square coils were considered, both with square cross section. Practical considerations such as wire selection, wire-wrapping efficiency, wire bending radius, choice of power supply, and inductance and time response were included. Using the equations provided in this paper, a designer can quickly design a set of tri-axial Helmholtz coils to generate a specified magnetic-field magnitude in the uniform-field region while maintaining specified accessibility to the central workspace.

ACKNOWLEDGMENTS

This research was supported in part by the National Science Foundation under Grant No. 1435827. The author would like to thank Alexandra Shamir for her assistance with Figures 3 and 5 and Dr. Andrew Petruska for many conversations about the design of electromagnets.

APPENDIX A: CONDUCTING AREA OF A SQUARE WIRE

The area of the square conductor with rounded corners shown in Fig. 1(b) can be solved as the superposition of the areas of two squares and one circle, as shown in Fig. 7. The area is calculated simply as

$$\text{area} = \delta_i^2 - (2\rho_i)^2 + \pi\rho_i^2 = \delta_i^2 - 0.8584\rho_i^2. \tag{A1}$$

This result is utilized in (2) and (25).

APPENDIX B: QUARTIC EQUATION OF X_c USED IN THE DESIGN OF CIRCULAR COILS

As described in Sec. IV, for the design of circular coils, solving for the parameter X_c for $c \in \{2,3\}$ involves solving for the roots of the quartic equation

$$a_4X_c^4 + a_3X_c^3 + a_2X_c^2 + a_1X_c + a_0 = 0 \tag{B1}$$

with coefficients

$$a_4 = 1.25\xi^2, \tag{B2}$$

$$a_3 = -5\xi^2\delta_o - 3\xi, \tag{B3}$$

$$a_2 = 7.5\xi^2\delta_o^2 + 6\xi\delta_o - 2T_c\xi - 4S_c\xi + 2, \tag{B4}$$

$$a_1 = -5\xi^2\delta_o^3 - 3\xi\delta_o^2 + 4(T_c + 2S_c)(\xi\delta_o + 1), \tag{B5}$$

$$a_0 = 1.25\xi^2\delta_o^4 - 2(T_c + 2S_c)\xi\delta_o^2 + 4(S_c^2 + T_c^2) - (G_{c-1} + 2X_{c-1} + 4T_{c-1})^2 - D_{oc-1}^2 \tag{B6}$$

with all parameters defined in Sec. IV.

An analytical solution for quartic equations exists, but the roots can also be found using numerical techniques. In our case, we should always expect to find a single positive real root among the four roots, which we return as our solution for X_c for the purpose of coil design.

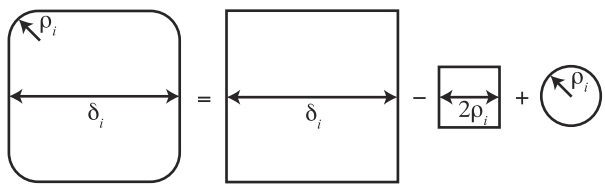

FIG. 7. The area of a square wire with inner (conductor) dimensions $\delta_i \times \delta_i$ and with corner radius-of-curvature ρ_i can be expressed as the superposition of the area of three simple geometries.

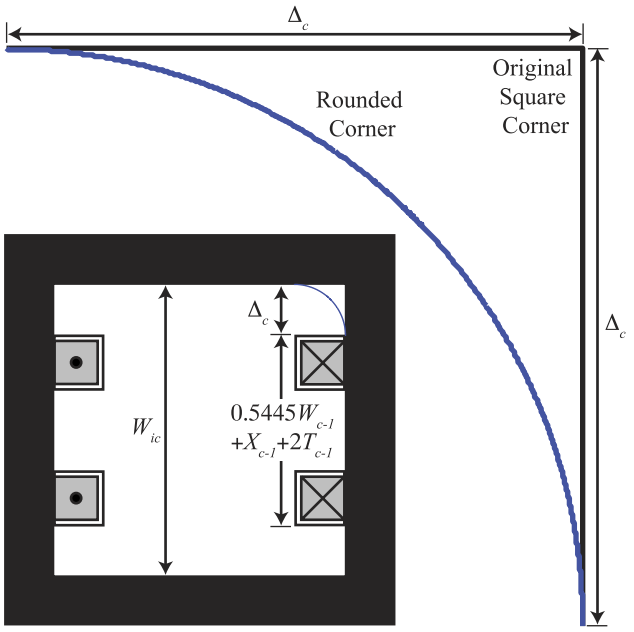

FIG. 8. When rounding the corners of square coils, the maximum allowable radius-of-curvature Δ_c for $c \in \{2,3\}$ is depicted.

APPENDIX C: UPPER LIMIT ON CORNER RADIUS FOR SQUARE COILS

For rounding the square corners of the middle and outer Helmholtz coils, the allowable radius-of-curvature Δ_c of the corner has an upper limit,

$$\Delta_c = 0.5(W_{ic} - (0.5445W_{c-1} + X_{c-1} + 2T_{c-1})) \quad \text{(C1)}$$

for $c \in \{2,3\}$, as depicted in Fig. 8. Choosing a radius-of-curvature larger than this value would result in the coils not nesting properly against each other; the nested parametric design described in Sec. V assumes that the portion of Helmholtz coil c that is in contact with Helmholtz coil $c-1$ is straight.

APPENDIX D: VALIDATION OF INDUCTANCE ESTIMATION METHOD

In Table III, we compare the estimated inductance using the method described in Sec. VI C 1 with experimentally measured values for a tri-axial circular Helmholtz coil set described by Mahoney *et al.*[14] However, note that the coils in that work were not designed using the methodology presented in this paper, so we explicitly use their reported values. Also note that the number of wraps wide reported was only accurate to the nearest integer, which constitutes approximately 5% uncertainty in the reported values. We find reasonable agreement between the reported values for inductance and our estimate and conclude that the estimation will be sufficient for the purposes of design.

TABLE III. Estimated inductance compared to measured values reported by Mahoney *et al.*[14] The number of wraps wide, deep, and the total wraps is reported per individual coil, whereas the inductance is reported for the pair connected in series. All coils are wrapped with round 14 AWG insulated copper magnet wire ($\delta_o = 1.628$ mm).

Coil pair c	D_c (mm)	Wraps wide	Wraps deep	Total wraps	Measured inductance (mH)	Estimated inductance (mH)
1	88	9	7	63	0.944	0.937
2	138	9	11	99	3.78	4.03
3	196	13	11	143	12.2	12.8

[1]A. E. Ruark and M. F. Peters, "Helmholtz coils for producing uniform magnetic fields," J. Opt. Soc. Am. **13**(2), 205–212 (1926).
[2]A. H. Firester, "Design of square Helmholtz coil systems," Rev. Sci. Instrum. **37**, 1264–1265 (1966).
[3]M. S. Crosser, S. Scott, A. Clark, and P. M. Wilt, "On the magnetic field near the center of Helmholtz coils," Rev. Sci. Instrum. **81**, 084701 (2010).
[4]R. K. Cacak and J. R. Craig, "Magnetic field uniformity around near-Helmholtz coil configurations," Rev. Sci. Instrum. **40**(11), 1468–1470 (1968).
[5]F. R. Crownfield, Jr., "Optimum spacing of coil pairs," Rev. Sci. Instrum. **35**, 240–241 (1964).
[6]M. E. Rudd and J. R. Craig, "Optimum spacing of square and circular coil pairs," Rev. Sci. Instrum. **39**, 1372–1374 (1968).
[7]P. A. Colavita and V. A. Bustos, "Optimum spacing for a pair of thick circular coils of square section," Rev. Sci. Instrum. **49**(7), 1006–1007 (1978).
[8]R. Grisenti and A. Zecca, "Design data for a triple square coil system," Rev. Sci. Instrum. **52**(7), 1097–1099 (1981).
[9]R. Merritt, C. Purcell, and G. Stroink, "Uniform magnetic field produced by three, four, and five square coils," Rev. Sci. Instrum. **54**(7), 879–882 (1983).
[10]E. M. Purcell, "Helmholtz coils revisited," Am. J. Phys. **57**(1), 18–22 (1989).
[11]E. Diller and M. Sitti, "Micro-scale mobile robotics," Found. Trends Rob. **2**(3), 143–259 (2013).
[12]B. J. Nelson, I. K. Kaliakatsos, and J. J. Abbott, "Microrobots for minimally invasive medicine," Annu. Rev. Biomed. Eng. **12**, 55–85 (2010).
[13]R. Beiranvand, "Magnetic field uniformity of the practical tri-axial Helmholtz coils systems," Rev. Sci. Instrum. **85**, 055115 (2014).
[14]A. W. Mahoney, J. C. Sarrazin, E. Bamberg, and J. J. Abbott, "Velocity control with gravity compensation for magnetic helical microswimmers," Adv. Rob. **25**, 1007–1028 (2011).
[15]H. A. Wheeler, "Simple inductance formulas for radio coils," Proc. Inst. Radio Eng. **16**(10), 1398–1400 (1928).
[16]F. W. Grover, *Inductance Calculations: Working Formulas and Tables* (Dover, 2004).